



ORIGINAL RESEARCH

Novel Acoustic Biomarker of Quality of Life in Left Ventricular Assist Device Recipients

Boyla O. Mainsah, PhD*; Priyesh A. Patel, MD*; Xinlin J. Chen , BS; Cameron Olsen, MD; Leslie M. Collins, PhD; Ravi Karra , MD, MHS

BACKGROUND: Although technological advances to pump design have improved survival, left ventricular assist device (LVAD) recipients experience variable improvements in quality of life. Methods for optimizing LVAD support to improve quality of life are needed. We investigated whether acoustic signatures obtained from digital stethoscopes can predict patient-centered outcomes in LVAD recipients.

METHODS AND RESULTS: We followed precordial sounds over 6 months in 24 LVAD recipients (8 HeartWare HVAD™, 16 HeartMate 3 [HM3]). Subjects recorded their precordial sounds with a digital stethoscope and completed a Kansas City Cardiomyopathy Questionnaire weekly. We developed a novel algorithm to filter LVAD sounds from recordings. Unsupervised clustering of LVAD-mitigated sounds revealed distinct groups of acoustic features. Of 16 HM3 recipients, 6 (38%) had a unique acoustic feature that we have termed the pulse synchronized sound based on its temporal association with the artificial pulse of the HM3. HM3 recipients with the pulse synchronized sound had significantly better Kansas City Cardiomyopathy Questionnaire scores at baseline (median, 89.1 [interquartile range, 86.2–90.4] versus 66.1 [interquartile range, 31.1–73.7]; $P=0.03$) and over the 6-month study period (marginal mean, 77.6 [95% CI, 66.3–88.9] versus 59.9 [95% CI, 47.9–70.0]; $P<0.001$). Mechanistically, the pulse synchronized sound shares acoustic features with patient-derived intrinsic sounds. Finally, we developed a machine learning algorithm to automatically detect the pulse synchronized sound within precordial sounds (area under the curve, 0.95, leave-one-subject-out cross-validation).

CONCLUSIONS: We have identified a novel acoustic biomarker associated with better quality of life in HM3 LVAD recipients, which may provide a method for assaying optimized LVAD support.

Key Words: acoustic analysis ■ biomarker ■ left ventricular assist device ■ mechanical circulatory support ■ precordial sounds ■ quality of life

Left ventricular assist devices (LVADs) are surgically implanted pumps that improve survival of patients with advanced heart failure.¹ Innovation to pump design over the past decade has resulted in more durable LVADs, with short-term survival rates now approaching heart transplantation.^{2–7} Although quality of life (QoL) generally improves after LVAD implantation, this response is heterogeneous.^{8–10} About 7.3% of LVAD recipients have persistently poor QoL indexes.^{11,12} Approaches to enhance QoL and reduce LVAD-related complications are needed to maximize

the effectiveness of LVAD support.¹³ A biomarker relating LVAD support to QoL could be an important clinical adjunct.

Since its invention by René Laennec in 1816, the stethoscope has been a staple of the bedside cardiovascular evaluation.

Advances in stethoscope design and the development of complimentary modalities have enabled the linkage of specific cardiac sounds to prognosis. For example, the S3 gallop is highly associated with decompensated heart failure, and acoustic surveillance

Correspondence to: Ravi Karra, MD, MHS, Duke University Medical Center, Box 102152, Durham, NC 27710, USA. E-mail: ravi.karra@duke.edu
Supplementary Material for this article is available at <https://www.ahajournals.org/doi/suppl/10.1161/JAHA.120.018588>

*Dr Mainsah and Dr Patel contributed equally to the manuscript.

For Sources of Funding and Disclosures, see page 10.

© 2021 The Authors. Published on behalf of the American Heart Association, Inc., by Wiley. This is an open access article under the terms of the Creative Commons Attribution-NonCommercial-NoDerivs License, which permits use and distribution in any medium, provided the original work is properly cited, the use is non-commercial and no modifications or adaptations are made.

JAHA is available at: www.ahajournals.org/journal/jaha

CLINICAL PERSPECTIVE

What Is New?

- A total of 24 left ventricular assist device recipients recorded their precordial sounds using digital stethoscopes and completed a Kansas City Cardiomyopathy Questionnaire, once a week for 6 months.
- We applied signal processing methods to recordings and identified a group of HeartMate 3 recipients with a shared pulse synchronized sound.
- HeartMate 3 recipients with the pulse synchronized sound have significantly better quality-of-life scores compared with HeartMate 3 recipients without the pulse synchronized sound.

What Are the Clinical Implications?

- The pulse synchronized sound has potential as a biomarker to identify optimized left ventricular assist device support in HeartMate 3 recipients.

Nonstandard Abbreviations and Acronyms

HM3	HeartMate 3
KCCQ	Kansas City Cardiomyopathy Questionnaire
PSS	pulse synchronized sound

for an S3 using implanted cardiac devices is a promising approach to identify patients at risk for decompensation.¹⁵ Auscultation of LVAD recipients, however, has unique challenges, with pump sounds often obscuring intrinsic cardiac sounds.

Signal processing is a field of electrical engineering that analyzes data representations of real-world signals, such as sound. Merging of signal processing techniques with machine learning has enabled the identification of acoustic features that can be incorporated into prediction tools. For example, digital media services analyze patterns of user preferences to predict content that a user may enjoy.¹⁶ As a running pump, the LVAD generates a characteristic acoustic spectrum determined by the rotational frequency of its impeller.¹⁷ Thus, disruptions of flow through the pump can cause changes to the distribution of acoustic spectral energy, and changes in the acoustic spectral pattern could be used to monitor pump function.¹⁷ In proof-of-concept work, we and others have determined that acute pump thrombosis

generates characteristic acoustic spectra, supporting our hypothesis that acoustic analysis can be used to monitor LVAD function and predict outcomes.^{18–20} Indeed, machine learning algorithms have been developed to detect suspected pump thrombosis using pump parameters and features extracted from precordial sounds.²¹ Herein, we have applied advanced signal processing techniques to digital sound recordings to identify a novel acoustic biomarker associated with improved QoL among LVAD recipients.

METHODS

Because of the sensitive nature of the data collected for this study, requests to access the data set from qualified researchers trained in human subject confidentiality protocols may be sent to Dr Karra.

Study Procedures

This study was approved by the Duke University Medical Center Institutional Review Board. Twenty-four patients from the Duke LVAD program were recruited, with a prespecified intention to enroll subjects supported by a HeartMate 3 (HM3; Abbott Laboratories) or a HeartWare HVAD (Medtronic, Inc) in a 2:1 ratio. After obtaining informed written consent, subjects were trained to record their precordial sounds from the left upper sternal border using a digital stethoscope (Thinklabs, LLC) connected to a digital recorder (Tascam). Subjects were instructed to perform 1-minute recordings weekly for 6 months. Data cards containing recordings were collected at routine 3- and 6-month follow-up appointments. In addition to recordings, subjects were e-mailed once a week with a link to complete a Kansas City Cardiomyopathy Questionnaire (KCCQ) to assess QoL.^{22,23} Clinical events were extracted and adjudicated by manual chart review. Data were collected and managed using Research Electronic Data Capture (REDCap), a secure Health Insurance Portability and Accountability Act–compliant web-based application.²⁴

Processing of Acoustic Data

Recordings were collected at a sampling rate of 44 100 Hz. As a preprocessing measure, the acoustic signals were bandpass filtered from 20 to 300 Hz to be within the expected frequency range of heart sounds.²⁵ Signals were then resampled at 600 Hz. An adaptive filter with a noise cancellation architecture using the normalized least-mean-squares algorithm was used to filter LVAD sounds from the precordial sound mixture.²⁶ Pump model-specific algorithms (Data S1) were used to estimate contributions of

LVAD sounds to the precordial sounds based on pump structure and speed.^{27,28} After adaptive filtering, acoustic features were extracted from the LVAD-mitigated precordial sounds and visualized with the uniform manifold approximation and projection algorithm (MATLAB Engine API for Python, MATLAB R2019a).^{29,30} The acoustic features were normalized power spectral densities within a frequency range of 20 to 300 Hz, estimated with the Welch method from 5-second recording segments.³¹ An unsupervised, 2-dimensional uniform manifold approximation and projection model was fit using power spectral features extracted from baseline recordings. This uniform manifold approximation and projection model was applied to transform features extracted from the remainder of the recordings over the 6-month period into the same space.

Statistical Analysis

Baseline continuous variables are displayed using the median with interquartile range (IQR), whereas categorical variables are summarized using counts with percentages for nonmissing variables. Comparisons between groups of participants with and without the acoustic biomarker were performed using the Wilcoxon rank-sum test or the χ^2 test for continuous and categorical variables, respectively (R v3.6.1).³² All reported *P* values are 2 sided.

To determine association of the acoustic biomarker with longitudinal KCCQ scores over time, we used a linear mixed effects model (lmerTest and emmeans packages, R) to account for repeated measures from the same subject and for missing observations.³³ The fixed effects included the biomarker group and time (in weeks) since enrollment. The random effect was survey time grouped by subject. The KCCQ score is a continuous variable ranging from 0 to 100, with higher values indicating better QoL.^{22,23} Time since enrollment was modeled as a continuous variable, whereas the pulse synchronized sound (PSS) group and subject identifier were modeled as categorical variables.

RESULTS

Study Participants

Baseline characteristics for study participants are listed in Table 1. Sixteen subjects were supported by an HM3 LVAD, and 8 subjects were supported by a HeartWare HVAD. The median age of the subjects was 67.5 years (IQR, 56.8–71.0 years). Eighty-three percent (20/24) of subjects were men. Fifty percent (12/24) of subjects had an underlying ischemic cardiomyopathy, and 8% (2/24) of subjects had a prior LVAD requiring exchange. The median duration of LVAD support was 646 days (IQR, 321–899 days). The median overall

KCCQ score for the cohort was 74.0 (IQR, 44.0–86.2). No subjects died during the study period or were lost to follow-up. One subject provided only a single recording. One subject underwent a pump exchange from an HVAD to an HM3, 17 weeks after enrollment.

A Novel Method to Mitigate LVAD Sounds From the Acoustic Spectrum of LVAD Recipients

Prior work using acoustic spectra of LVAD recipients to identify pump thrombosis has largely focused on LVAD-derived sounds. However, clinical assessments of LVAD function consider parameters that reflect the patient-pump interaction, such as left ventricular dimension, the frequency of aortic valve opening, and the degree of mitral regurgitation. Accordingly, we reasoned that analyses enriched for patient-derived intrinsic heart sounds could be valuable for monitoring LVAD recipients. To enrich for intrinsic heart sounds, we leveraged knowledge of the different time-frequency characteristics of LVAD sounds to develop a novel adaptive filtering pipeline for mitigating LVAD sounds in the precordial sound mixture. Clustering of acoustic features extracted from precordial sounds before adaptive filtering was primarily driven by pump-related frequency components, with mostly subject-specific clusters and clusters with subjects having similar pump speeds (Figure S1). In contrast, clustering of acoustic features extracted from LVAD-mitigated sounds after adaptive filtering resulted in fewer clusters, indicating similarities of residual sounds (some independent of pump type) between LVAD recipients (Figure 1A).

To further verify that our adaptive filtering algorithm could enrich for patient-derived intrinsic sounds, we recorded precordial sounds from hospitalized LVAD recipients during a clinically indicated echocardiogram-guided ramp study (Data S1). We used contemporaneous echocardiographic images to annotate sound recordings with temporal markers of the cardiac cycle. On the basis of these annotations and time-frequency analysis, we were able to: (i) match the timing of S1 obtained from the echocardiogram to corresponding peaks in the LVAD-mitigated sounds; and (ii) determine that the frequency ranges of these peaks were within those of heart sounds (Figure S2). Together, these results indicate the robustness of our approach to enrich for intrinsic patient-derived sounds.

Unsupervised Clustering of LVAD-Mitigated Sounds Identifies a Unique Cluster of HM3 Recipients

As a first-pass analysis, we sought to determine how similar LVAD-mitigated precordial sounds

Table 1. Characteristics of the Study Population

Characteristic*	Overall (n=24)	No PSS (n=10)	PSS (n=6)	P Value†
Demographics, vitals				
Age, median (IQR), y	68 (57–71)	68 (62–71)	70 (64–73)	0.48
Male sex, n (%)	20 (83)	8 (80)	5 (83)	1.00
Weight, median (IQR), lb	230 (189–246)	245 (199–267)	198 (188–214)	0.22
MAP, median (IQR), mm Hg	82 (72–100)	97 (81–109)	85 (70–92)	0.16
Ventricular assist device				
HM3, n (%)	16 (67)	10 (100)	6 (100)	...
HVAD™, n (%)	8 (33)			
Time since implant, median (IQR), d	646 (321–899)	472 (300–720)	543 (306–648)	0.87
Speed, HM3, median (IQR), rpm	5600 (5475–5700)	5650 (5600–5775)	5350 (5225–5625)	0.05
Speed, HeartWare HVAD™, median (IQR), rpm	2970 (2900–2985)			
Flow, median (IQR), L/min	4.6 (4.3–4.8)	4.7 (4.4–4.9)	4.2 (3.9–4.6)	0.17
Power, median (IQR), W	...	4.4 (4.2–4.6)	4.0 (3.9–4.1)	0.01
PI, HM3, median (IQR)	3.9 (2.8–5.1)	4.2 (2.7–4.5)	3.6 (3.4–6.2)	0.91
Cardiac function				
LVEF, median (IQR), %	20 (15–20)	20 (16–28)	18 (15–20)	0.22
LVEDD, median (IQR), cm	5.5 (5.0–6.5)	5.5 (4.2–6.7)	5.3 (5.0–5.8)	0.79
Valve function				
Aortic valve opening, n (%)				0.45
Every beat	5 (21)	1 (10)	3 (50)	
Intermittent	3 (13)	1 (10)	1 (17)	
Immobile	12 (50)	6 (60)	2 (33)	
Mitral regurgitation, n (%)				0.59
None	6 (25)	4 (40)	2 (33)	
Trivial	8 (33)	3 (30)	3 (50)	
Mild	6 (25)	0 (0)	1 (17)	
Moderate	3 (13)	2 (20)	0	
Severe	0 (0)	0	0	
Functional capacity				
NYHA classification, n (%)				0.54
Class I	7 (29)	2 (20)	3 (50)	
Class II	13 (54)	5 (50)	2 (33)	
Class III	4 (17)	3 (30)	1 (17)	
Class IV	0 (0)	0 (0)	0 (0)	
Baseline KCCQ score, median (IQR)	74 (44–86)	66.1 (31.1–73.7)	89.1 (86.2–90.4)	0.03
Comorbidities, n (%)				
COPD	6 (25)	3 (30)	1 (17)	1.00
Diabetes mellitus	9 (38)	6 (60)	2 (33)	0.61
Ischemic cardiomyopathy	12 (50)	4 (40)	5 (83)	0.15
History of CVA/TIA	6 (25)	2 (20)	2 (33)	0.60
History of gastrointestinal hemorrhage	7 (29)	3 (30)	2 (33)	1.00
History of LVAD thrombosis	3 (13)	0 (0)	3 (50)	0.04
History of LVAD driveline infection	1 (4)	1 (10)	0 (0)	1.00
Concomitant medication, n (%)				
β-Blocker	14 (58)	5 (50)	5 (83)	0.31
ACE inhibitor, ARB, or ARNI	13 (54)	4 (40)	4 (67)	0.61
Aldosterone antagonist	20 (83)	8 (80)	6 (100)	0.50

(Continued)

Table 1. Continued

Characteristic*	Overall (n=24)	No PSS (n=10)	PSS (n=6)	P Value†
Loop diuretic	21 (88)	8 (80)	5 (83)	1.00
Other antihypertensive	10 (42)	4 (40)	2 (33)	1.00
Baseline laboratory data				
Serum sodium, median (IQR), mmol/L	138 (136–139)	138 (136–138)	137 (135–139)	0.96
Blood urea nitrogen, median (IQR), mg/dL	19 (15–24)	20 (17–31)	16 (14–22)	0.16
Serum creatinine, median (IQR), mg/dL	1.3 (1.1–1.5)	1.4 (1.2–1.7)	1.1 (1.0–1.3)	0.25
Hemoglobin, median (IQR), g/dL	13.8 (11.6–14.3)	13.4 (10.5–14.3)	14.1 (13.2–14.2)	0.66
Total bilirubin, median (IQR), mg/dL	0.8 (0.7–1.0)	0.7 (0.5–0.8)	1.0 (0.8–1.1)	0.07
No. of unplanned hospitalizations, median (IQR)	0.5 (0–2)	0.5 (0–1.75)	0 (0–0.75)	0.44

ACE indicates angiotensin-converting enzyme; ARB, angiotensin receptor blocker; ARNI, angiotensin receptor–neprilysin inhibitor; COPD, chronic obstructive pulmonary disease; CVA, cerebrovascular accident; HM3, HeartMate 3; IQR, interquartile range; KCCQ, Kansas City Cardiomyopathy Questionnaire; LVAD, left ventricular assist device; LVEDD, left ventricular end-diastolic dimension; LVEF, left ventricular ejection fraction; MAP, mean arterial pressure; NYHA, New York Heart Association; PI, pulsatility index; PSS, pulse synchronized sound; and TIA, transient ischemic attack.

*Data reported as median (25th–75th percentile) or count (percentage).

†Comparisons were done using either the Wilcoxon rank-sum test or the χ^2 test for continuous and categorical variables, respectively.

were between subjects using baseline recordings. We performed unsupervised clustering of spectral features extracted from baseline LVAD-mitigated precordial sounds that yielded 8 distinct clusters (Figure 1A) and summarized the clusters by their dominant frequency characteristics (Figure S3). Inspection of the power spectra revealed that various levels of artifact led to the clustering of most sounds. Sources of artifact in noise-related clusters included equipment-related noise (clusters 1, 2, and 7) and high-amplitude residual pump-related frequency components (clusters 3 and 8). The rest of the clusters were dominated by sounds with frequency characteristics suggestive of heart and lung sounds (clusters 4, 5, and 6).^{25,34} However, one cluster stood out because it was entirely composed of subjects with an HM3 LVAD (cluster 6).

To better understand the shared acoustic features within clusters, we inspected the corresponding time-domain signals of the LVAD-mitigated precordial sounds (Figure 1B through 1D). We noted that the signals in cluster 6 had a “triple-peak” morphological feature that recurred every 2 seconds, which was not present in other HM3 recipients (Figure 1C and 1D). Unlike other LVADs, the HM3 undergoes a programmed speed oscillation every 2 seconds, termed an “artificial pulse,” to wash the impeller²⁷; thus, the timing of the triple peak seemed to reflect that of this artificial pulse. To associate the triple peak with the artificial pulse, we developed an algorithm to automatically identify the occurrence of the artificial pulse in precordial sounds. Strikingly, the triple peak was coincident with the artificial pulse (Figure 1D). On the basis of its temporal association with the artificial pulse, we termed the triple peak the “PSS.”

We initially suspected that the PSS was a sound generated by the LVAD, based on its temporal

relationship with the artificial pulse of the HM3, and analyzed spectrograms to confirm our hypothesis. Spectrograms are used in signal processing to visualize the relative intensity of frequency characteristics of signals as they vary over time. Because LVADs have a set speed, LVAD sounds are characterized by discrete frequency components at a fundamental frequency ($f = \frac{\text{revolutions per minute}}{60 \text{ seconds/minute}} \text{ Hz}$) and their harmonics. Harmonics are particularly prominent at multiples of the blade pass frequency ($f_{bp} = b \times f \text{ Hz}$), where b is the number of blades of the pump. During the artificial pulse of the HM3, the pump speed undergoes 3 changes: it decreases by 2000 revolutions per minute (rpm) for 0.15 seconds, increases by 4000 rpm for 0.2 seconds, and then decreases by 2000 rpm to return to the set speed.²⁷ These oscillations would be expected to result in frequency shifts of 33 Hz (2000 rpm/60 s/min) relative to the fundamental frequency of the set speed. The spectrogram of an HM3 would thus be expected to have a horizontal band at the fundamental frequency of the set speed with frequency shifts of 33 Hz during the artificial pulse (Figure S4). A similar pattern would be expected for each harmonic. Surprisingly, when we analyzed spectrograms from subjects with the PSS, we noted that the PSS occurred predominantly within a frequency range of 20 to 100 Hz (Figure 2), which is more characteristic of intrinsic heart sounds.^{25,34} In addition, the high-intensity energy bursts of the PSS during the artificial pulse are transient, have a wider bandwidth than pump-derived sounds, and do not exhibit 33-Hz shifts (Figure 2H), demonstrating that PSS features do not completely mirror what would be expected from an entirely LVAD derived sound (Figure S4). Together, our findings suggest that the PSS results from an interaction of the patient and pump during the artificial pulse.

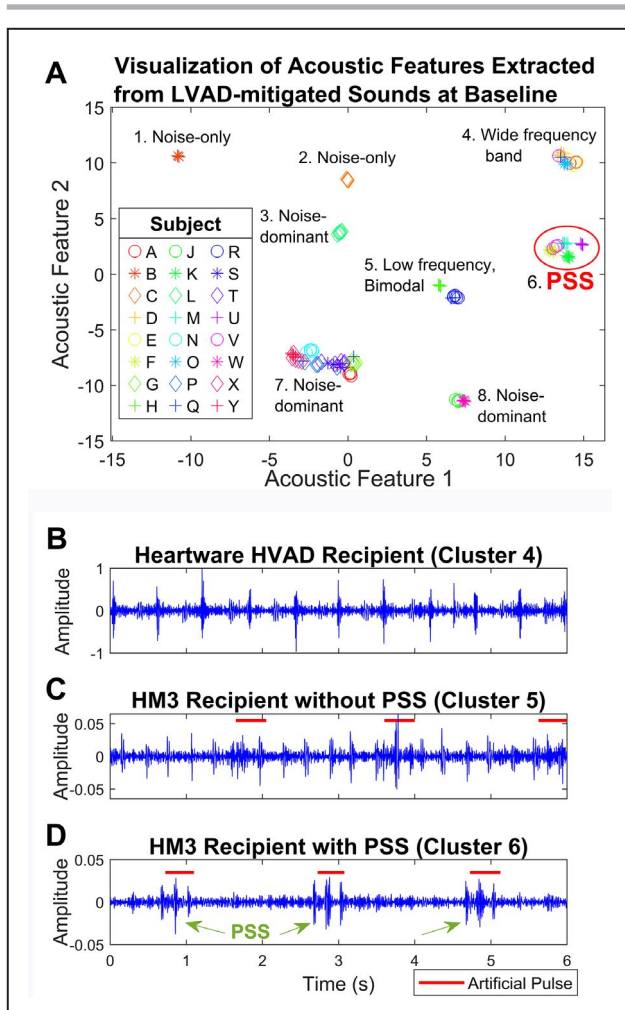


Figure 1. Unsupervised clustering of left ventricular assist device (LVAD)-mitigated sounds.

A, Unsupervised clustering of baseline LVAD-mitigated sounds. Each scatter point represents a power spectral density feature within a range of 20 to 300 Hz extracted from a 5-second segment. Clusters are annotated with their dominant frequency characteristics; the cluster dominated by the pulse synchronized sound (PSS) is indicated with the red circle. **B to D**, Representative time-domain signals from clusters with frequency characteristics similar to those of patient-derived sounds. A 6-second interval of LVAD-mitigated sounds is shown for the indicated clusters. Compared with HeartMate 3 (HM3) recipients without the PSS (**C**), HM3 recipients with the PSS (**D**) have a characteristic “triple peak” (green arrows) that occurs every 2 seconds, synchronized with the artificial pulse (red lines) of the HM3.

The PSS Marks HM3 Recipients With Better QoL Scores

We next performed unsupervised clustering of the LVAD-mitigated precordial sounds over the entire 6-month study period and once again identified a unique cluster of subjects with the PSS (Figure 3A). As might be expected of subject-acquired data, the sound recordings were of variable quality, evident by the amount of data in the noise-related clusters. We used knowledge about the time-frequency characteristics of

the different noise types to identify recordings of sufficient quality for analysis (Data S1 and Table S1). Fifty-five percent (353/640) of recordings over 6 months passed quality control. From the resulting data set, we found that 38% (6/16) of HM3 recipients had the PSS. All subjects (4/4) who had the PSS in their baseline recording and who submitted longitudinal recordings continued to have the PSS over the entire study period. One subject who did not have the PSS at baseline had the PSS in additional recordings over the 6-month period; review of this subject’s baseline data indicated a low-quality recording. Overall, after excluding data of poor quality, only 21.2% (24/113) of recordings over 6 months for subjects with the PSS did not contain observable PSS, demonstrating the reproducibility of this finding over time.

To better understand the clinical significance of the PSS, we first compared the baseline characteristics of HM3 recipients with and without the PSS (Table 1). At baseline, subjects with the PSS were grossly similar to subjects without the PSS, except for having lower pump power (median, 4.0 W [IQR, 3.9–4.1 W] versus 4.4 W [IQR, 4.2–4.6 W]; 2-sided $P=0.01$) and a significantly higher overall KCCQ QoL score (median, 89.1 [IQR, 86.2–90.4] versus 66.1 [IQR, 31.1–73.7]; 2-sided $P=0.03$) (Table 1). In addition, subjects with the PSS tended to have lower set speeds (median, 5350 rpm [IQR, 5225–5625 rpm] versus 5650 rpm [IQR, 5600–5775 rpm]; 2-sided $P=0.05$), lower pump flow (median, 4.2 L/min [IQR, 3.9–4.6 L/min] versus 4.7 L/min [IQR, 4.4–4.9 L/min]; 2-sided $P=0.17$), and lower mean arterial pressures (median, 85 mm Hg [IQR, 70–92 mm Hg] versus 97 mm Hg [IQR, 81–109 mm Hg]; 2-sided $P=0.16$), although none of these differences met statistical significance (Table 1). When we evaluated the longitudinal relationship of KCCQ score to the presence of the PSS in HM3 recipients (Figure 3B), we found the presence of the PSS to be highly associated with better QoL over time, even after adjusting for repeated measures (estimated marginal mean, 77.6 [95% CI, 66.3–88.9] versus 59.9 [95% CI, 47.9–70.0]; $P<0.001$ for the pairwise comparison; Table 2). We next explored the relationship between the PSS and other clinical events. Although subjects with the PSS had fewer unplanned hospitalizations, this result was not significant (median, 0 [IQR, 0–0.75] versus 0.5 [IQR, 0–1.75]; 2-sided $P=0.44$; Table 1). Thus, the PSS is likely to mark a subset of HM3 recipients with better QoL and potentially a more benign clinical course.

The PSS Can Be Reliably Detected Using an Acoustic Classifier

Because identification of the PSS is dependent on advanced signal processing techniques to mitigate LVAD sounds, the PSS cannot easily be identified on routine

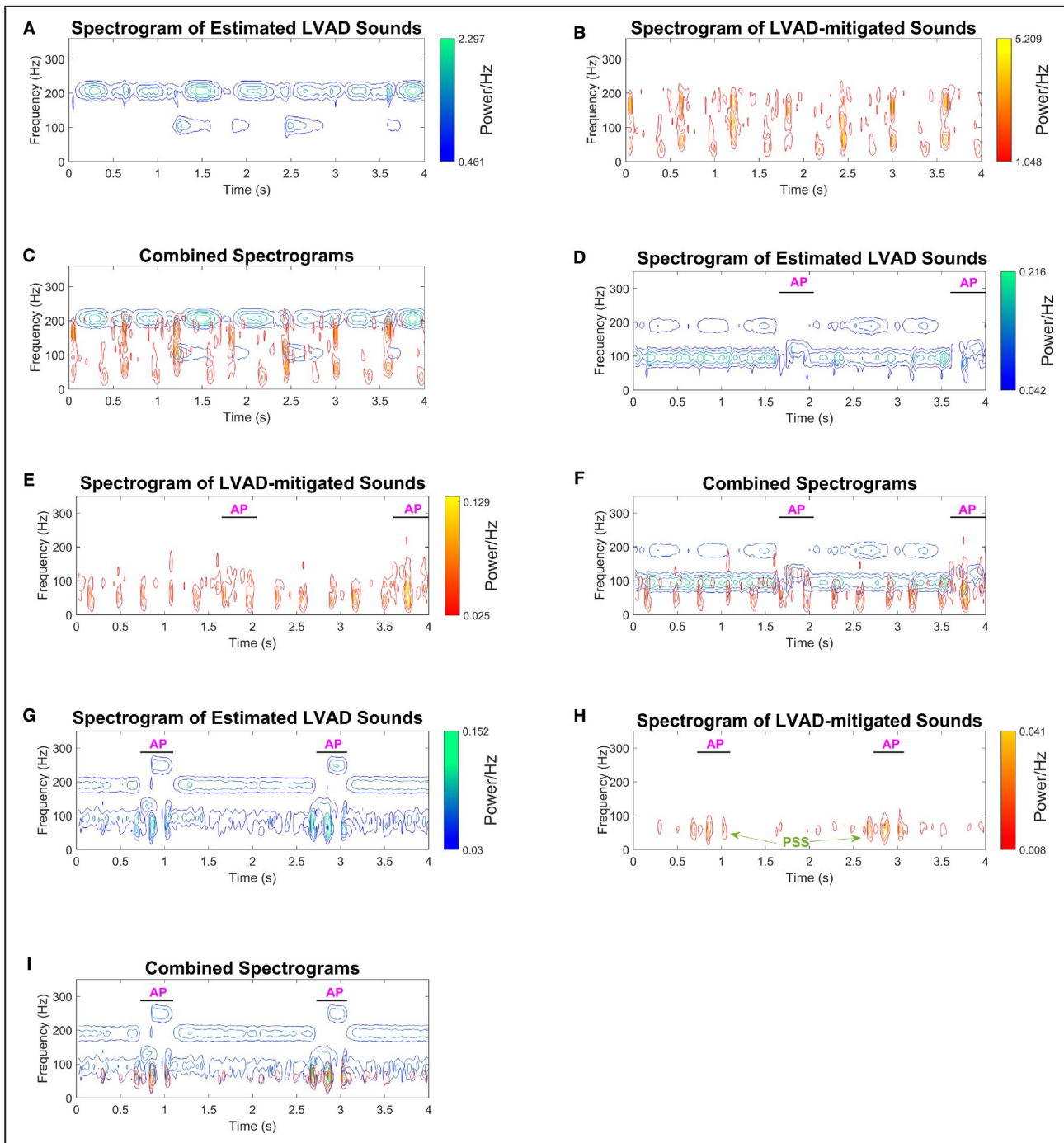


Figure 2. Spectrograms of estimated left ventricular assist device (LVAD) sounds and LVAD-mitigated precordial sounds. **A to C**, Spectrograms for a subject with a HeartWare HVAD™. **D to F**, Spectrograms for a subject with a HeartMate 3 (HM3) without the pulse synchronized sound (PSS). **G to I**, Spectrograms for a subjects with an HM3 with the PSS. The frequency content of the LVAD sound is characterized by discrete peaks in the frequency domain at multiples of the pump's fundamental frequency, which can be observed as horizontal lines (**A**, **D**, and **G**), with shifts attributable to speed changes during the artificial pulse of the HM3 (**D** and **G**). Estimates of LVAD sounds obtained from adaptive filtering may contain residual non-LVAD sound components when there is frequency overlap. In HM3 recipients without the PSS (**E**), the peaks of the LVAD-mitigated sounds are not in phase with the artificial pulse (AP), whereas in HM3 recipients with the PSS (**H**, **I**), the triple peaks are in phase with the AP.

auscultation. Thus, use of the PSS requires a robust machine learning algorithm to reliably detect its presence within precordial sounds. Toward this end, we took advantage of the alignment of the PSS with the

artificial pulse of the HM3 to develop acoustic features aligned with the time segments of the artificial pulse. We then trained a support-vector machine classifier with these features and evaluated performance with a

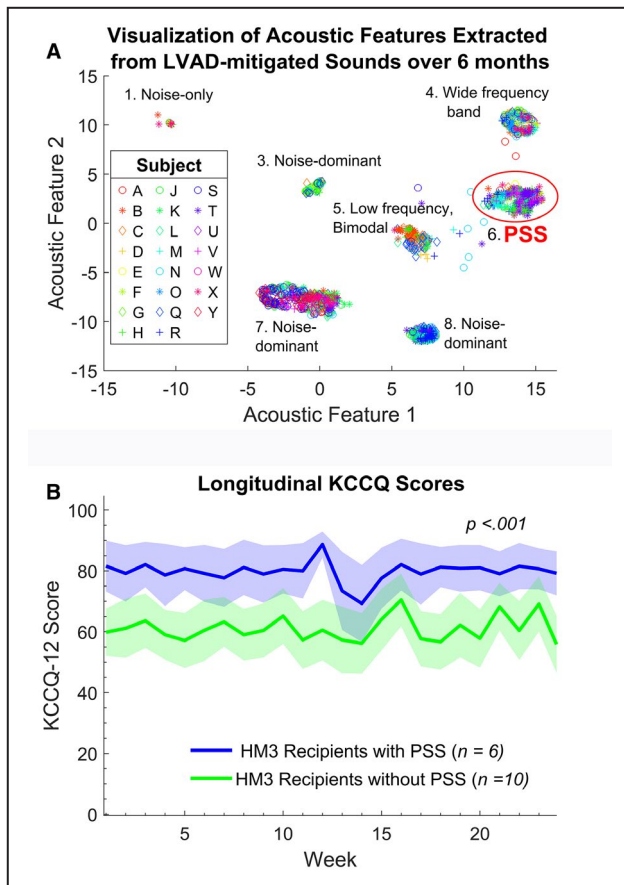


Figure 3. Longitudinal assessment of the pulse synchronized sound (PSS).

A, Unsupervised clustering of left ventricular assist device (LVAD)-mitigated sounds collected over 6 months. Each scatter point represents a power spectral density feature within a range of 20 to 300 Hz extracted from a 5-second segment. Clusters are annotated with their dominant characteristics; the cluster dominated by the PSS is indicated with the red circle. **B**, Longitudinal Kansas City Cardiomyopathy Questionnaire (KCCQ) scores of HeartMate 3 (HM3) LVAD recipients with and without the PSS. The solid line and shaded region represent the mean and SEM, respectively, for each group. Analysis with a linear mixed-effects model revealed a significant association of the PSS with KCCQ scores ($P < 0.001$).

leave-one-subject-out training and testing approach. We were able to develop a classifier to identify the PSS with an area under the receiver operating characteristic of 0.95, sensitivity of 0.91, and specificity of 0.88 at the optimal threshold (Figure 4). False negatives (9.2% of the training data set) were largely related to obfuscation of the PSS by breathing artifact, whereas false positives (3.45% of the data set) were largely related to overlap of innate heart sounds with the PSS.

DISCUSSION

LVADs have transformed the care of patients with advanced heart failure but continue to be associated

with high rates of morbidity and frequent unplanned hospitalizations. Efforts to mitigate LVAD-related morbidity are critical for enhancing the effectiveness of LVAD support.¹³ Reengineering LVADs to be more durable and less thrombogenic has partially addressed this need, but additional strategies are needed.^{2-4,35} Specifically, key questions remain about the optimization of pump speed and pharmacologic therapy in LVAD recipients.³⁶ Indeed, recent work has suggested that optimizing pump support using invasive hemodynamics can reduce the number of unplanned hospitalizations.³⁷ However, the invasive nature of catheterization, along with the requirement for specialized clinical settings, limits the utility of this approach. By contrast, noninvasive markers of LVAD efficacy could be readily incorporated in the bedside assessment of LVAD recipients and even remotely by patients themselves.

We performed a prospective, observational study and identified an acoustic biomarker in a subset of HM3 recipients that we have termed the PSS. The PSS is highly reproducible and is strongly associated with better QoL scores. The 23-point difference in median KCCQ score in subjects with the PSS compared with subjects without the PSS is consistent with a large clinical difference.²³ Although the PSS can be assessed with digital stethoscopes, signal processing techniques are required to facilitate its detection within precordial sounds. Accordingly, we have developed a classifier to accurately detect the PSS. Such a classifier can be incorporated into mobile applications, as has been recently done for detection of pathologic murmurs.³⁸ Extra heart sounds have classically been associated with cardiovascular pathological features; however, the PSS, to our knowledge, is the first acoustic biomarker to be associated with a favorable response to LVAD support. Although we observed fewer, nonsignificant, unplanned hospitalizations in subjects with the PSS, we had a low overall rate of unplanned hospitalizations in our cohort. Larger studies are needed to determine whether this biomarker also associates with better clinical outcomes.

Prior work using acoustics for monitoring LVAD function has largely focused on pump thrombosis.¹⁸⁻²¹ Most of these studies analyzed the amplitudes of harmonics of the fundamental LVAD frequency, essentially focusing on LVAD-specific sounds.¹⁸⁻²⁰ By contrast, we have developed a novel method to enrich for non-LVAD precordial sounds. Our approach is unique and has the potential to assess the physiologic interaction of the recipient with the LVAD. We analyzed time-frequency representations of LVAD-mitigated sounds and used prior knowledge of pump sounds and intrinsic heart sounds to determine the likely source of the PSS. Surprisingly, although the PSS is temporally associated with the artificial pulse of the HM3, the frequency domain of the PSS is more consistent with sounds

Table 2. Linear Mixed-Effects Model for Association of Longitudinal KCCQ Scores With the PSS

Fixed Effects	β Estimate	SE	95% CI	P Value
Intercept	61.07	1.69	57.75 to 64.38	<0.001
Time (week)	-0.17	0.43	-1.02 to 0.68	0.69
PSS group*	18.69	2.75	13.32 to 24.08	<0.001
Random Effects	σ Estimate		95% CI	
Time	1.62		1.13 to 2.33	
PSS Group	EM Mean	SE	95% CI	
No PSS	58.93	5.22	47.85 to 70.02	
PSS	77.62	5.39	66.30 to 88.94	
Pairwise Comparison	Estimate	SE	P Value	
No PSS–PSS	-18.70	2.76	<0.001	

Model included 16 participants and 334 observations and was adjusted by subject. Time was treated as a continuous variable, whereas subject and the PSS group were treated as categorical variables. The random effect of time was grouped by subject. Results for coefficients of fixed factors and estimates for random factors are shown. Estimated marginal means and associated pairwise comparison for subjects with and without the PSS are also shown. EM indicates estimated marginal; KCCQ, Kansas City Cardiomyopathy Questionnaire; and PSS, pulse synchronized sound.

*Referenced from the group without the PSS.

originating from the patient.²⁵ Because the HM3 artificial pulse occurs by rapid oscillations in the pump speed, we conjecture that the PSS reflects an optimized degree of ventricular unloading or remodeling such that these speed oscillations reverberate through the myocardium or vasculature. In vitro modeling of flow through the HM3 suggests that the artificial pulse results in rapid changes to flow velocity and pressure

gradients within the pump.³⁹ Clinically, these rapid flow variations during the artificial pulse are often manifest by an increase in the LVAD inflow velocity that can be transmitted to the peripheral vasculature as a palpable pulse.^{40,41} Of the myocardium and the vasculature, the frequency range of the PSS (20–100 Hz) is closer to the range of a myocardial sound, compared with arterial wall vibrations that generate higher-frequency sounds.^{25,42–45} If the PSS is indicative of an optimized interface of recipient and LVAD, assaying for the PSS may be useful for tuning LVAD speeds or pharmacologic therapy. However, additional investigations of the mechanism of the PSS, and whether interventions can be linked to the PSS, are needed.

Although our study demonstrated a proof of principle, we acknowledge key limitations. First, our biomarker is specific to patients supported by an HM3 LVAD. Larger studies will be needed to determine whether similar acoustic biomarkers are present with other LVAD types. However, since commercial approval, the HM3 has become the most common type of implanted durable LVAD,⁴⁶ suggesting that our finding has broad relevance. Second, we observed that data quality was limited by noise in 45% (287/640) of recordings. Better acoustic sensors with improved noise immunity, such as implanted sensors, could alleviate this limitation. Other limitations include the small sample size and possible selection bias of our study. Subjects were selected from a group of stable outpatients with the ability to perform digital recordings (median duration of support, 646 days [IQR, 321–899 days]). Such a selection could have enriched our population for responders to LVAD support, leading to an enrichment of high QoL scores in our cohort. However, the KCCQ scores of our HM3 population (median overall KCCQ

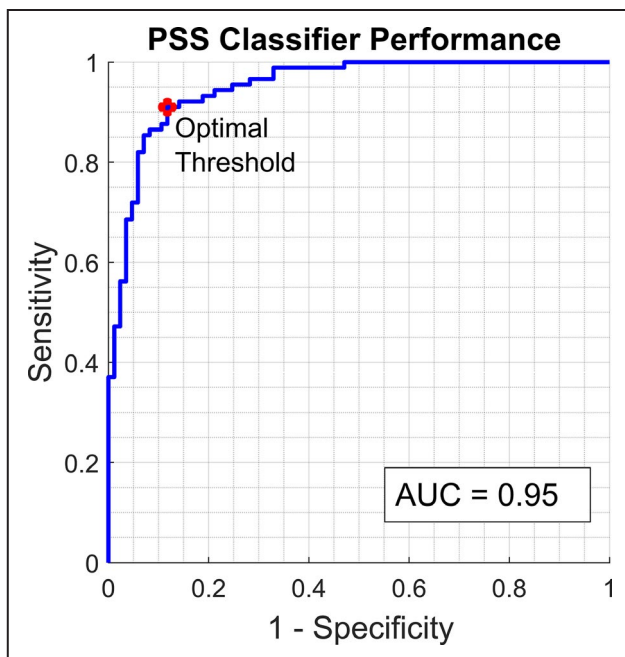


Figure 4. Receiver operating characteristic and area under the curve (AUC) for a support vector machine classifier to detect the pulse synchronized sound (PSS).

The classifier was trained with leave-one-subject-out cross-validation. The operating point associated with the optimal threshold to minimize the probability of error is indicated.

score, 72.4 [IQR, 40.9–88.8]) compared favorably with the overall KCCQ score of HM3 recipients in the The Multicenter Study of MagLev Technology in Patients Undergoing Mechanical Circulatory Support Therapy with HeartMate 3 (MOMENTUM 3) trial at 3 (median KCCQ score of 68) and 6 months (median KCCQ score of 69).⁹ Future work in a larger cohort of LVAD recipients can address these limitations.

In summary, we have applied signal processing and machine learning methods to routine clinical auscultation to identify a new acoustic biomarker of QoL in LVAD recipients. Future work will determine whether this biomarker can be used to optimize LVAD support. Although focused on LVAD recipients, the approach and method used herein are broadly applicable and can lead to the discovery of a new class of clinically significant acoustic biomarkers from complex sound mixtures.

ARTICLE INFORMATION

Received July 21, 2020; accepted January 8, 2021.

Affiliations

From the Department of Electrical and Computer Engineering, Duke University, Durham, NC (B.O.M., X.J.C., L.M.C.); Sanger Heart and Vascular Institute, Atrium Health, Charlotte, NC (P.A.P.); and Division of Cardiology, Department of Medicine, Duke University Medical Center, Durham, NC (C.O., R.K.).

Acknowledgments

The authors would like to thank Ms Laura Blue and Dr Han Billard at the Duke Left Ventricular Assist Device Clinic for their clinical research support, and Mr William Ratliff at the Duke Institute for Health Innovation for his project management support. We would also like to thank Drs Thomas Bashore and Stuart Russell for their helpful comments.

Author contributions: Dr Karra provided oversight for all aspects of the study. Drs Karra, Mainsah, Patel, and Collins designed the study. Dr Mainsah, X.J. Chen, and Dr Collins developed algorithms and code for processing recordings. Drs Patel, Olsen, and Karra collected and analyzed clinical data. Dr Mainsah, X.J. Chen, Dr Patel, Dr Olsen, and Dr Karra performed statistical analysis. Dr Mainsah, X.J. Chen, and Dr Karra wrote the manuscript, with feedback from all the other coauthors.

Sources of Funding

This study was funded by a grant from the Duke Institute for Health Innovation. Mr Clive Smith and Thinklabs Medical, LLC, provided digital stethoscopes and technical support. Support for the Duke Office of Clinical Research to host REDCap was made possible by grant UL1TR001117 from the National Center for Research Resources, a component of the National Institutes of Health (NIH), and NIH Roadmap for Medical Research. Dr Karra was additionally supported by a Duke Strong Start Physician Scientist Award.

Disclosures

Drs Mainsah, Patel, Collins, and Karra and X.J. Chen have filed provisional patent applications around the signal processing algorithm, the pulse synchronized sound, and its detection. Dr Karra reports a research grant from Abbott Laboratories. The remaining authors have no disclosures to report.

Supplementary Material

Data S1

Table S1

Figures S1–S4

REFERENCES

- Kirklın JK, Pagani FD, Kormos RL, Stevenson LW, Blume ED, Myers SL, Miller MA, Baldwin JT, Young JB, Naftel DC. Eighth annual INTERMACS report: special focus on framing the impact of adverse events. *J Heart Lung Transplant*. 2017;36:1080–1086. DOI: 10.1016/j.healun.2017.07.005.
- Mehra MR, Uriel N, Naka Y, Cleveland JC Jr, Yuzefpolskaya M, Salerno CT, Walsh MN, Milano CA, Patel CB, Hutchins SW, et al. A fully magnetically levitated left ventricular assist device - final report. *N Engl J Med*. 2019;380:1618–1627. DOI: 10.1056/NEJMoa1900486.
- Mehra MR, Naka Y, Uriel N, Goldstein DJ, Cleveland JC Jr, Colombo PC, Walsh MN, Milano CA, Patel CB, Jorde UP, et al. A fully magnetically levitated circulatory pump for advanced heart failure. *N Engl J Med*. 2017;376:440–450. DOI: 10.1056/NEJMoa1610426.
- Mehra MR, Goldstein DJ, Uriel N, Cleveland JC Jr, Yuzefpolskaya M, Salerno C, Walsh MN, Milano CA, Patel CB, Ewald GA, et al. Two-year outcomes with a magnetically levitated cardiac pump in heart failure. *N Engl J Med*. 2018;378:1386–1395. DOI: 10.1056/NEJMoa1800866.
- Slaughter MS, Rogers JG, Milano CA, Russell SD, Conte JV, Feldman D, Sun B, Tatooles AJ, Delgado RM III, Long JW, et al. Advanced heart failure treated with continuous-flow left ventricular assist device. *N Engl J Med*. 2009;361:2241–2251. DOI: 10.1056/NEJMoa090938.
- Rogers JG, Pagani FD, Tatooles AJ, Bhat G, Slaughter MS, Birks EJ, Boyce SW, Najjar SS, Jeevanandam V, Anderson AS, et al. Intra-pericardial left ventricular assist device for advanced heart failure. *N Engl J Med*. 2017;376:451–460. DOI: 10.1056/NEJMoa1602954.
- Lund LH, Khush KK, Cherikh WS, Goldfarb S, Kucheryavaya AY, Levvey BJ, Meiser B, Rossano JW, Chambers DC, Yusef RD. The registry of the International Society for Heart and Lung Transplantation: thirty-fourth adult heart transplantation report—2017; focus theme: allograft ischemic time. *J Heart Lung Transpl*. 2017;36:1037–1046. DOI: 10.1016/j.healun.2017.07.019.
- Brouwers C, Denollet J, De Jonge N, Caliskan K, Kealy J, Pedersen SS. Patient-reported outcomes in left ventricular assist device therapy: a systematic review and recommendations for clinical research and practice. *Circ Heart Fail*. 2011;4:714–723. DOI: 10.1161/CIRCHEARTF.A119.962472.
- Cowger JA, Naka Y, Aaronson KD, Horstmannshof D, Gulati S, Rinde-Hoffman D, Pinney S, Adatya S, Farrar DJ, Jorde UP, et al. Quality of life and functional capacity outcomes in the momentum 3 trial at 6 months: a call for new metrics for left ventricular assist device patients. *J Heart Lung Transplant*. 2018;37:15–24. DOI: 10.1016/j.healun.2017.10.019.
- Rogers JG, Aaronson KD, Boyle AJ, Russell SD, Milano CA, Pagani FD, Edwards BS, Park S, John R, Conte JV, et al. Continuous flow left ventricular assist device improves functional capacity and quality of life of advanced heart failure patients. *J Am Coll Cardiol*. 2010;55:1826–1834. DOI: 10.1016/j.jacc.2009.12.052.
- Fendler TJ, Nassif ME, Kennedy KF, Joseph SM, Silvestry SC, Ewald GA, LaRue SJ, Vader JM, Spertus JA, Arnold SV. Global outcome in patients with left ventricular assist devices. *Am J Cardiol*. 2017;119:1069–1073. DOI: 10.1016/j.amjcard.2016.12.014.
- Arnold SV, Jones PG, Allen LA, Cohen DJ, Fendler TJ, Holtz JE, Aggarwal S, Spertus JA. Frequency of poor outcome (death or poor quality of life) after left ventricular assist device for destination therapy: results from the InterMACS Registry. *Circ Heart Fail*. 2016;9:e002800.
- Baras Shreibati J, Goldhaber-Fiebert JD, Banerjee D, Owens DK, Hlatky MA. Cost-effectiveness of left ventricular assist devices in ambulatory patients with advanced heart failure. *JACC Heart Fail*. 2017;5:110–119. DOI: 10.1016/j.jchf.2016.09.008.
- Laennec RTH. De L'auscultation Médiate: Ou, Traité Du Diagnostic Des Maladies Des Poumons Et Du Coeur; Fondé Principalement Sur Ce Nouveau Moyen D'exploration. Culture Et Civilisation. Paris, France: Brosson et Chaudé; 1819.
- Boehmer JP, Hariharan R, Devecchi FG, Smith AL, Molon G, Capucci A, An Q, Averina V, Stolen CM, Thakur PH, et al. A multisensor algorithm predicts heart failure events in patients with implanted devices: results from the Multisense Study. *JACC Heart Fail*. 2017;5:216–225. DOI: 10.1016/j.jchf.2016.12.011.
- Kaplan A, Haenlein M. Siri, Siri, in my hand: who's the fairest in the land? On the interpretations, illustrations, and implications of artificial intelligence. *Bus Horiz*. 2019;62:15–25.
- Norton MP, Karczub DG. *Fundamentals of Noise and Vibration Analysis for Engineers*. Cambridge, UK; New York, NY: Cambridge University Press; 2003.
- Patel P, Mainsah B, Milano CA, Nowacek DP, Collins L, Karra R. Acoustic signatures of left ventricular assist device thrombosis. *J Eng Sci Med Diagn Ther*. 2019;2:024501.

19. Yost GI, Royston TJ, Bhat G, Tatooles AJ. Acoustic characterization of axial flow left ventricular assist device operation in vitro and in vivo. *Asaio J*. 2016;62:46–55. DOI: 10.1097/MAT.0000000000000307.
20. Kaufmann F, Hormandinger C, Stepanenko A, Kretzschmar A, Soltani S, Krabatsch T, Potapov E, Hetzer R. Acoustic spectral analysis for determining pump thrombosis in rotary blood pumps. *ASAIO J*. 2014;60:502–507. DOI: 10.1097/MAT.0000000000000097.
21. Semiz B, Hersek S, Pouyan MB, Partida C, Arroyo LB, Selby V, Wieselthaler G, Rehj J, Klein L, Inan O. Detecting suspected pump thrombosis in left ventricular assist devices via acoustic analysis. *IEEE J Biomed Health Inform*. 2020;24:1899–1906. DOI: 10.1109/JBHI.2020.2966178.
22. Green CP, Porter CB, Bresnahan DR, Spertus JA. Development and evaluation of the Kansas city cardiomyopathy questionnaire: a new health status measure for heart failure. *J Am Coll Cardiol*. 2000;35:1245–1255. DOI: 10.1016/S0735-1097(00)00531-3.
23. Spertus J, Peterson E, Conard MW, Heidenreich PA, Krumholz HM, Jones P, McCullough PA, Pina I, Tooley J, Weintraub WS, et al. Monitoring clinical changes in patients with heart failure: a comparison of methods. *Am Heart J*. 2005;150:707–715. DOI: 10.1016/j.ahj.2004.12.010.
24. Harris PA, Taylor R, Thielke R, Payne J, Gonzalez N, Conde JG. Research Electronic Data Capture (Redcap)—a metadata-driven methodology and workflow process for providing translational research informatics support. *J Biomed Inform*. 2009;42:377–381. DOI: 10.1016/j.jbi.2008.08.010.
25. Dwivedi AK, Imtiaz SA, Rodriguez-Villegas E. Algorithms for automatic analysis and classification of heart sounds—a systematic review. *IEEE Access*. 2019;7:8316–8345. DOI: 10.1109/ACCESS.2018.2889437.
26. Widrow B, Glover JR, McCool JM, Kaunitz J, Williams CS, Hearn RH, Zeidler JR, Eugene Dong JR, Goodlin RC. Adaptive noise canceling: principles and applications. *Proc IEEE*. 1975;63:1692–1716. DOI: 10.1109/PROC.1975.10036.
27. Thoratec Corporation. Introduction: Heartmate 3 Left Ventricular Assist System Instructions for Use. Pleasanton, CA: Thoratec Corporation; 2018.
28. Heartware, Inc. Principles of Operation. Heartware Ventricular Assist System: Instructions for Use. Miami Lakes, FL: HeartWare, Inc.; 2012.
29. McInnes L, Healy J, Saul N, Großberger L. UMAP: uniform manifold approximation and projection. *J Open Source Softw*. 2018;3:861. DOI: 10.21105/joss.00861.
30. McInnes L, Healy J, Saul N, Großberger L. UMAP: uniform manifold approximation and projection. *J Open Source Softw*. 2018;3:861. DOI: 10.21105/joss.00861.
31. Welch P. The use of fast Fourier transform for the estimation of power spectra: a method based on time averaging over short, modified periodograms. *IEEE Trans Audio Electroacoust*. 1967;15:70–73. DOI: 10.1109/TAU.1967.1161901.
32. R Core Team. *R: A language and environment for statistical computing*. Vienna, Austria: R Foundation for Statistical Computing; 2013. Available at: <https://www.R-project.org/>.
33. Gałecki A, Burzykowski T. *Linear mixed-effects model. Linear Mixed-Effects Models Using R: A Step-by-Step Approach*. New York, NY: Springer; 2013:245–273.
34. Rao A, Huynh E, Royston TJ, Kornblith A, Roy S. Acoustic methods for pulmonary diagnosis. *IEEE Rev Biomed Eng*. 2018;12:221–239. DOI: 10.1109/RBME.2018.2874353.
35. Mehra MR, Salerno C, Cleveland JC, Pinney S, Yuzefpolskaya M, Milano CA, Itoh A, Goldstein DJ, Uriel N, Gulati S, et al. Healthcare resource use and cost implications in the momentum 3 Long-Term Outcome Study. *Circulation*. 2018;138:1923–1934. DOI: 10.1161/CIRCULATIONAHA.118.035722.
36. Kirklin JK, Pagani FD, Goldstein DJ, John R, Rogers JG, Atluri P, Arabia FA, Cheung A, Holman W, Hoopes C, et al. American Association for Thoracic Surgery/International Society for Heart and Lung Transplantation guidelines on selected topics in mechanical circulatory support. *J Heart Lung Transplant*. 2020;39:187–219. DOI: 10.1016/j.healun.2020.01.1329.
37. Imamura T, Nguyen A, Kim G, Raikhelkar J, Sarswat N, Kalantari S, Smith B, Juricek C, Rodgers D, Ota T, et al. Optimal haemodynamics during left ventricular assist device support are associated with reduced haemocompatibility-related adverse events. *Eur J Heart Fail*. 2019;21:655–662. DOI: 10.1002/ejhf.1372.
38. Lin Y-J, Chuang C-W, Yen C-Y, Huang P-W, Huang P-W, Chen J-Y, Lee S-Y. An intelligent stethoscope with ECG and heart sound synchronous display. 2019 IEEE International Symposium on Circuits and Systems (ISCAS). 2019:1–4.
39. Wiegmann L, Thamsen B, De Zelicourt D, Granegger M, Boes S, Schmid Daners M, Meboldt M, Kurtcuoglu V. Fluid dynamics in the Heartmate 3: influence of the artificial pulse feature and residual cardiac pulsation. *Artif Organs*. 2019;43:363–376. DOI: 10.1111/aor.13346.
40. Essandoh M, Essandoh G, Stallkamp ED, Perez WJ. Spectral Doppler analysis of the HeartMate 3 left ventricular assist device inflow: new challenges presented by the artificial pulse technology. *J Cardiothorac Vasc Anesth*. 2018;32:e4–e5. DOI: 10.1053/j.jvca.2018.07.005.
41. Castagna F, Stöhr EJ, Pinsino A, Cockcroft JR, Willey J, Reshad Garan A, Topkara VK, Colombo PC, Yuzefpolskaya M, McDonnell BJ. The unique blood pressures and pulsatility of LVAD patients: current challenges and future opportunities. *Curr Hypertens Rep*. 2017;19:85. DOI: 10.1007/s11906-017-0782-6.
42. Kistler J, Lees R, Friedman J, Pressin M, Mohr J, Roberson G, Ojemann R. The bruit of carotid stenosis versus radiated basal heart murmurs: differentiation by phonoangiography. *Circulation*. 1978;57:975–981. DOI: 10.1161/01.CIR.57.5.975.
43. Lees RS. Phonoangiography: qualitative and quantitative. *Ann Biomed Eng*. 1984;12:55–62. DOI: 10.1007/BF02410291.
44. Foreman JE, Hutchison KJ. Arterial wall vibration distal to stenoses in isolated arteries of dog and man. *Circ Res*. 1970;26:583–590. DOI: 10.1161/01.RES.26.5.583.
45. Miller A, Lees RS, Kistler JP, Abbott WM. Effects of surrounding tissue on the sound spectrum of arterial bruits in vivo. *Stroke*. 1980;11:394–398. DOI: 10.1161/01.STR.11.4.394.
46. Teuteberg JJ, Cleveland JC, Cowger J, Higgins RS, Goldstein DJ, Keebler M, Kirklin JK, Myers SL, Salerno CT, Stehlik J. The Society of Thoracic Surgeons Intermacs 2019 Annual Report: the changing landscape of devices and indications. *Ann Thorac Surg*. 2019;2020:649–660. DOI: 10.1016/j.athoracsur.2019.12.005.

SUPPLEMENTAL MATERIAL

Data S1.

Supplemental Methods

I. Adaptive Filtering of LVAD-generated Sounds

The frequency spectrum of LVAD-generated sounds is characterized by peaks at multiples, or *harmonics*, of the pump's *fundamental* frequency, f . The fundamental frequency of the pump, expressed in Hertz (Hz), is determined accordingly:¹⁷

$$f = \frac{r}{60}, \quad (1)$$

where r corresponds to pump's rotational speed, in revolutions per minute (rpm). Peaks are also expected at harmonics of the blade passing frequency, f_{bp} , which are determined accordingly:¹⁷

$$f_{bp} = b \times f, \quad (2)$$

where b is the number of impeller blades in the pump.

The HM3 and HVAD are both centrifugal-flow pumps with four impeller blades (i.e., $b = 4$).^{27, 28} The HVAD is programmed to operate at a constant pump speed. In contrast, the HM3 employs an “*artificial pulse*” (AP) feature and is programmed to undergo pump speed changes from the set speed every two seconds: dropping by 2000 rpm for 0.15 seconds (s), then increasing by 4000rpm for 0.2s, before returning to the primary speed. The speed changes during the AP in the HM3 generate LVAD sounds with short bursts of energy at the *secondary* frequencies.

Recorded precordial sounds in LVAD recipients contain a mixture of LVAD sounds and intrinsic sounds. An adaptive filter with a noise cancellation architecture employing the normalized least-mean-squares algorithm was used to separate LVAD sounds from intrinsic precordial sounds.²⁶ Noise references simulating expected LVAD sounds were employed to adaptively estimate the contributions of the LVAD sounds in the precordial sound mixture. These noise references were generated

using sinusoids at frequencies corresponding to harmonics of the pump's fundamental frequency. For HM3 LVAD recipients, the adaptive filtering methodology was modified; primary and secondary pump frequencies were filtered using separate noise references.

II. Quality Assessment of Recordings

As might be expected of subject-acquired data, the sound recordings were of variable quality. Predominant acoustic artifact included equipment-related noise due to user-error and ambient noise, such as voices. Equipment-related noise sources were identified by replicating user-error scenarios, which included: incomplete insertion of the audio jack into the recorder (cluster 1, Figure 1A); a powered-off digital stethoscope (cluster 2, Figure 1A); and application of pressure on the head of the digital stethoscope (cluster 7, Figure 1A). Recordings with no audio signals due to a powered-off digital stethoscope were denoted as *noise-only* recordings, while recordings with the other equipment-related noise types were denoted as *noisy* recordings (**Table S1**). We used knowledge about the time-frequency characteristics of the different noise types to identify recordings of sufficient quality (55% of recordings) for analysis.

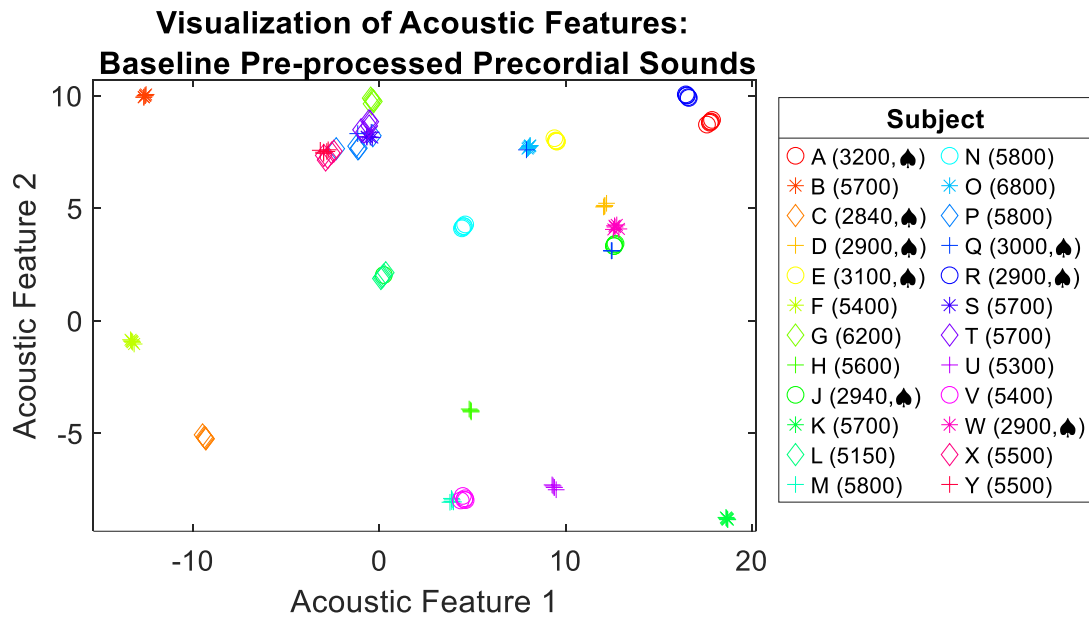
III. Ramp Study Protocol

Hospitalized participants were approached at the time of their clinically indicated echocardiography-guided ramp study for LVAD speed optimization. After written informed consent was obtained, echocardiographic loops and digital recordings were acquired at each speed. Recordings were then manually synchronized with echocardiographic loops using mitral valve closure as landmarks (**Figure S2**).

Table S1. Summary of Recordings by Subject.

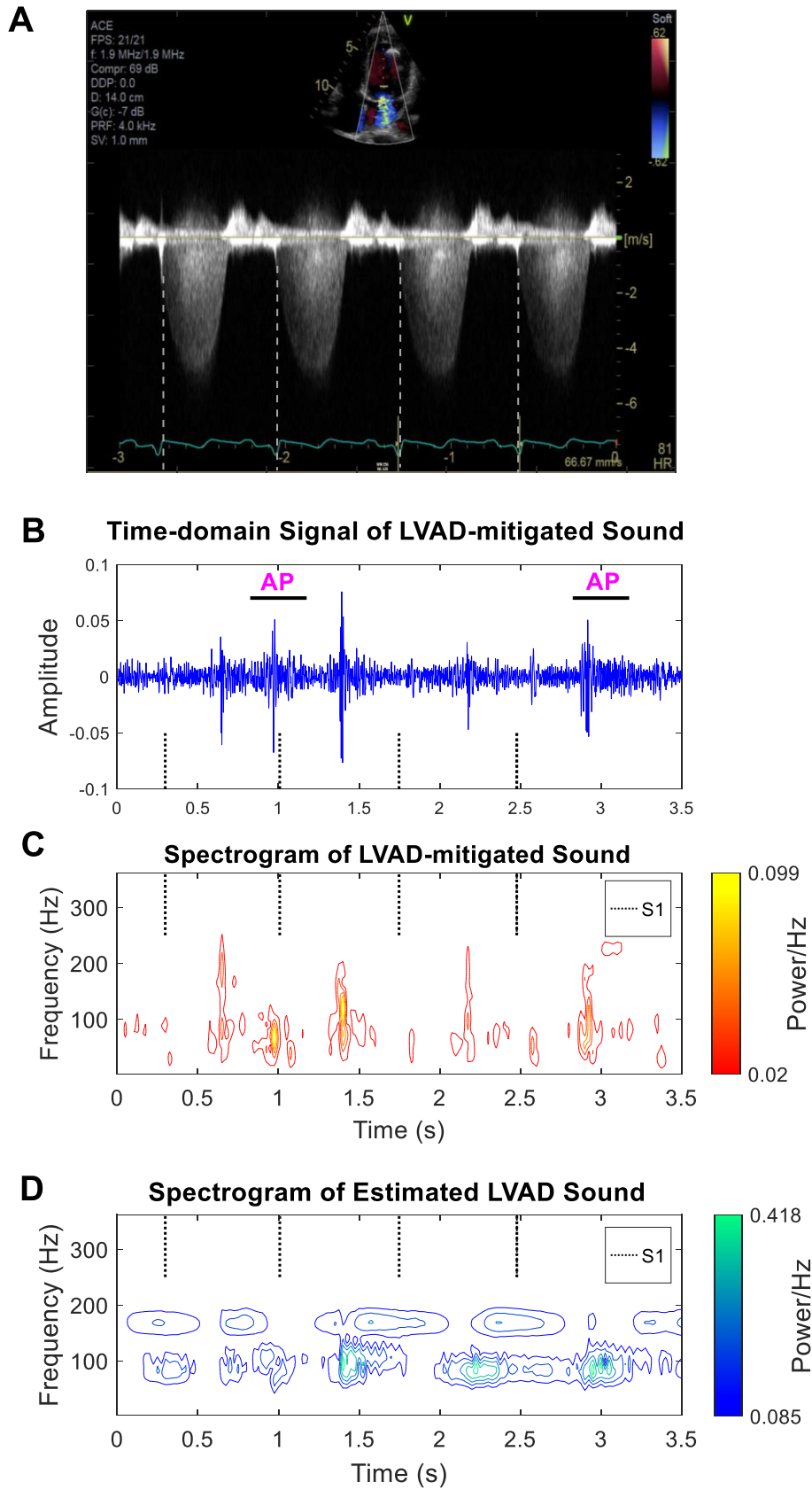
Subject	LVAD Model	Total Number of Recordings	Number of Recordings with Sufficient Quality (Recordings with PSS)	Number of Recordings < 25 seconds	Number of Noise-only (NO) or Noisy (N) Recordings		Number of Weekly Surveys Completion (out of 24)
					NO	N	
A	HVAD	8	8	0	0	0	11
B	HM3	33	24	1	6	2	24
C	HVAD	28	11	3	8	4	20
D	HVAD	16	10	3	1	1	16
E	HVAD	26	26	0	0	0	24
F	HM3	35	16 (11)	5	10	5	24
G	HM3	26	10	2	0	14	20
H	HM3	39	32	2	3	2	24
J	HVAD	27	14	1	0	12	24
K	HM3	33	23 (23)	2	3	5	24
L	HM3	17	6	0	1	10	17
M	HM3	31	19 (8)	1	1	10	24
N	HM3	32	4	3	0	25	24
O	HM3	29	26	1	2	0	24
P	HM3	25	1	7	17	0	18
Q	HVAD	24	14	1	2	5	17
R	HVAD	27	25	1	1	0	24
S	HM3	28	4	1	1	22	24
T	HM3	30	27 (27)	0	1	2	24
U	HM3	2	1 (1)	1	0	0	3
V	HM3	36	27 (20)	2	1	6	24
W	HVAD	28	1	0	27	0	24
X	HM3	30	24	0	3	4	24
Y	HM3	30	0	1	5	24	100
Total		640	353	38	93	153	

Figure S1. Unsupervised clustering of baseline recordings prior to adaptive filtering of left ventricular assist device (LVAD) sounds.



Each scatter point represents a power spectral density feature within a range of 20-300 Hz computed from a 5-second segment. The LVAD pump speed (revolutions per minute) for each subject is indicated in parentheses. Subjects had either a Heartware HVAD (indicated with '♠' symbol) or Heartmate 3 (HM3) LVAD.

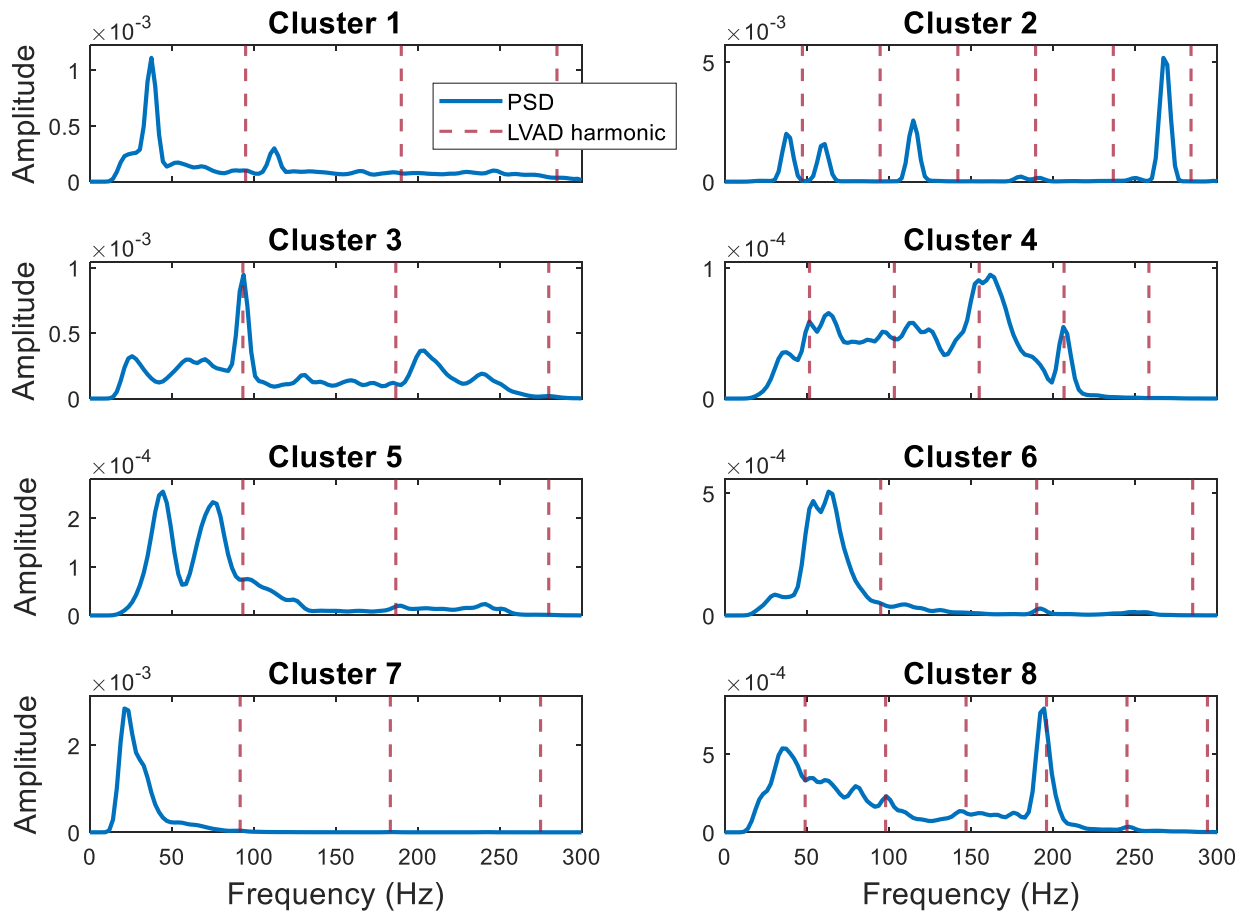
Figure S2. Adaptive filtering of left ventricular assist device (LVAD) sounds enriches for intrinsic sounds.



Simultaneously acquired

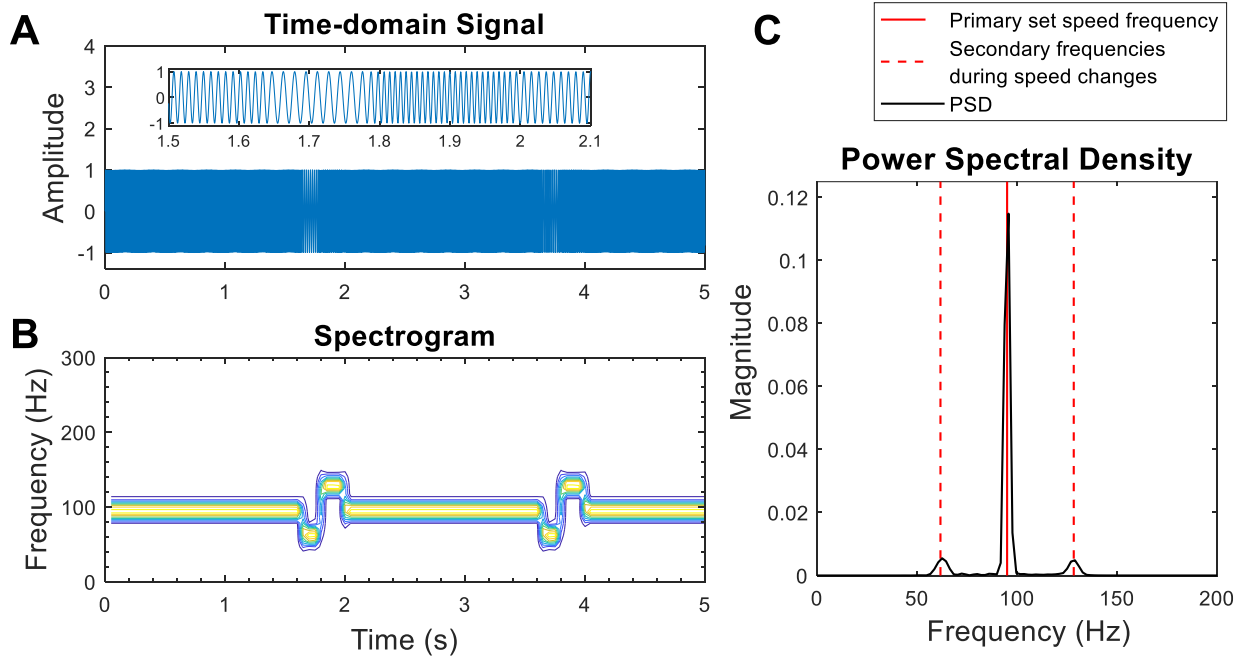
echocardiograms and precordial sound recordings were used to register acoustic features with mitral valve closure. For this subject, at this set speed of 5000 revolutions per minute (rpm), the aortic valve opened with every beat. **A**, Continuous wave Doppler of the mitral inflow. **B**, Time domain signal of LVAD-mitigated precordial sounds. Spectrogram showing frequency content of **C**, LVAD-mitigated precordial sounds and **D**, estimated LVAD sounds. Estimated frequency domains for LVAD sounds and LVAD-mitigated sounds are annotated. Heatmap indicates the relative intensity of the acoustic frequency content. Dashed vertical lines correspond to S1 based on the mitral inflow pattern (**A**) and correlate with high amplitude signals (**B**) that are in the frequency range of intrinsic heart sounds (**C**).

Figure S3. Representative power spectral densities (PSDs) from clusters of left ventricular assist device (LVAD)-mitigated sounds.



Harmonics of the primary pump speed are indicated by dashed lines. The clusters are characterized by: (1) equipment-related noise due to incomplete insertion of the audio jack in the recorder; (2) equipment-related noise due to a powered-off digital stethoscope; (3) a residual low frequency LVAD harmonic at 93.33 Hz; (4) a wide frequency band; (5) a low frequency, bimodal band; (6) a low frequency, pulse-synchronized sound; (7) low frequency equipment-related noise due to application of pressure on the head of the digital stethoscope; and (8) a residual high frequency LVAD harmonic at 194.5 Hz.

Figure S4. Predicted changes in acoustic features during the artificial pulse (AP) of the Heartmate 3 (HM3).



Pump sounds can be modeled with a sinusoid with the frequency, f , determined by the pump speed. Every 2 seconds, the HM3 speed decreases by 2000 revolutions (rpm) for 0.15 seconds, increases by 4000 rpm for 0.2 seconds, and then decreases by 2000 rpm to return to the set speed.²⁷ **A**, Time-domain signal with a magnified inset of the frequency changes ($f \pm 33.33$ Hz) during the AP, **B**, spectrogram and **C**, power spectral density (PSD) estimate for a pump with a set speed of 5700 rpm, resulting in a fundamental frequency of 95 Hz.